Available online at www.sciencedirect.com
ScienceDirect
Electrochimica Acta 53 (2007) 700–709
ELECTROCHIMICA Acta
www.elsevier.com/locate/electacta

Investigation of hydrogen adsorption–absorption on iron by EIS

N. Amokrane, C. Gabrielli *, E. Ostermann, H. Perrot

UPR15-CNRS, LISE, Université Pierre et Marie Curie, 4 Place Jussieu, 75252 Paris Cedex 05, France

Received 18 January 2007; received in revised form 19 July 2007; accepted 21 July 2007
Available online 27 July 2007

Abstract

This work concerns the interaction between hydrogen and iron in the cathodic potential region. It was motivated by the need for a better understanding of the hydrogen insertion mechanism in metals. Electrochemical deposits of iron with various thicknesses were carried out on a gold substrate and they were characterized by impedance measurements under hydrogen evolution conditions.

The processes occurring at the surface and within the iron films deposited on a gold electrode were studied using various electrochemical techniques. The impedance and voltammetric behaviours were strongly dependent on the film thickness. The main result of this study is that the charge transfer resistance increases with the film thickness. A model of the adsorption–absorption of hydrogen into iron films was proposed. It considered two types of absorbed hydrogen in a sublayer richer in hydrogen than the bulk metal. There, the hydrogen transported in the film coexists with another one coming from a direct absorption mechanism and "trapped" in some sites. The two absorbed hydrogen are reversibly exchanged. The interaction of hydrogen with palladium and iron was compared. It was concluded that for iron, the insertion of hydrogen results from a competition between a one-step direct hydrogen absorption mechanism and the classical two-step indirect penetration in the metal via the adsorbed hydrogen. At the end, a possible explanation of the deep penetration of the direct hydrogen absorption in the metal, detected by the impedance analysis, is proposed. It is based on the imperfections of numerous first layers of the deposited metals on polycrystalline gold.

Keywords: Hydrogen; Iron; Adsorption; Absorption; Impedance

1. Introduction

Numerous studies about hydrogen interaction with metals have been carried out because of their potential interest in various industrial domains. Hydrogen absorbing materials are important in hydrogen storage, metal-hydride batteries, and fuel cells. On the other hand, problems of degradation of steel may occur when hydrogen is in contact with some materials. This phenomenon, called hydrogen embrittlement, is frequently encountered in industrial environment. Hydrogen can penetrate in a metal by a physical process under high pressure or more often under an electrochemical driving force. Corrosion, cathodic protection of steel in sea water produces hydrogen. This production of hydrogen is also involved during steel production under hydrogenated environment, in storage and use of this gas or storage and transport of products which can, by decomposition, produce hydrogen (natural gas, oil, corrosive products, etc.). This hydrogen enters and diffuses into steel structure and this insertion creates constraints, which induce defects or cracks in the material.

The adsorption–desorption coupling has been studied thoroughly for the hydrogen/palladium system, which is known to store hydrogen in two possible phases depending on the cathodic potential: the α-PdH phase (0.02 hydrogen atom per Pd atom) and the β-phase (up to 0.6 hydrogen atom per Pd atom). Pyun and yang [1], have considered the interstitial sites in the β-phase and phase boundaries between the α and β phases as reversible and irreversible trap sites, respectively, which follow a McNabb and Foster model [2]. They have also proposed that a thin β-PdH phase layer, sometimes in patches, between the electrode surface and subsurface give rise to the predominant direct hydrogen absorption reaction and acts as a barrier for hydrogen diffusion [3]. On similar basis, Gabrielli et al. have proposed a model, in terms of impedances measured on thin Pd films deposited on gold, where, in parallel with the classical Volmer–Heyrovsky absorption two-step mechanism [4], trapped hydrogen atoms, located in a thin subsurface layer, may exchange charge directly with protons of the solution [5,6]. More recently, Lasia et al.

* Corresponding author. Tel.: +33 144274136; fax: +33 144274074.
E-mail address: cg@ccr.jussieu.fr (C. Gabrielli).

0013-4686/$ – see front matter © 2007 Elsevier Ltd. All rights reserved.
doi:10.1016/j.electacta.2007.07.047

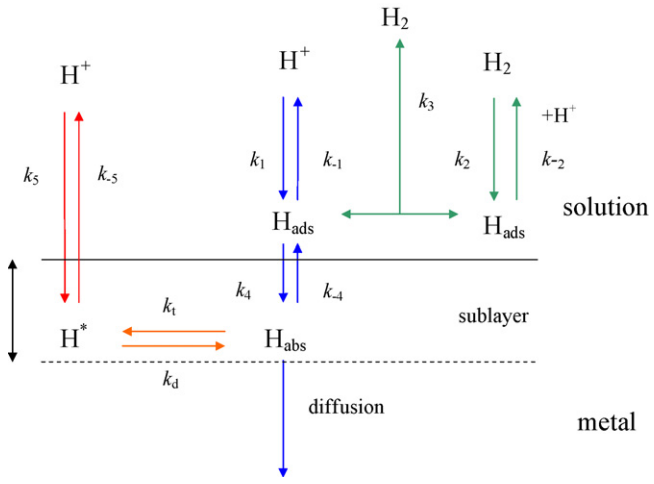

Fig. 1. Scheme of the reaction mechanism used for the general interaction of hydrogen with a metal.

have shown, for very thin films (0.8–10 monolayers) of palladium, that two parallel mechanisms participate to hydrogen entry in the metal: a fast direct hydrogen absorption and a slower indirect hydrogen absorption via an adsorption step [7–9].

As a first step, in order to understand hydrogen insertion mechanism, the interaction between hydrogen and iron was studied as this material is easier to manipulate than steel, in particular to deposit thin layers on a gold substrate, which blocks hydrogen penetration. Iron deposits with various thicknesses were electrochemically deposited and characterized by impedance measurements. The experimental approach was inspired by the results of electrochemical measurements recently obtained for the hydrogen/palladium system [4,5]. They have shown the importance of surface processes on the insertion kinetics of hydrogen in palladium. An investigation with respect to the material thickness has been necessary to separate the surface processes from the volume processes.

In spite of the numerous studies carried out on the iron/hydrogen system [10–14], many problems remain open. In addition, few investigations have been carried out by using impedance measurements, which is a very powerful tool to separate the various processes involved in complex reaction mechanisms.

In this paper, a model of the mechanism of hydrogen penetration in iron under cathodic polarization was proposed. Then, results obtained by voltammetry and impedance measurements concerning the interaction of hydrogen with thin films of iron deposited on a gold substrate were reported and compared with the model predictions.

2. Theory

2.1. Electrochemical mechanism

Usually, hydrogen atoms are considered to enter the metal either by a two-step (indirect) or a direct absorption mechanism. Equations below are written assuming that the two processes occur in parallel, which is schematized in Fig. 1.

The first step of the indirect absoprtion is hydrogen adsorption (Volmer reaction), with rate v_1

$$H^+ + M + e^- \underset{k_{-1}}{\overset{k_1}{\rightleftarrows}} MH_{ads} + H_2O \quad (1)$$

where M is the adsorption site on the metal surface and MH_{ads} is the hydrogen atom adsorbed on the electrode surface.

Adsorbed hydrogen can form gaseous hydrogen by the two following processes:

(i) electrochemical desorption (Heyrovsky reaction), with rate v_2:

$$MH_{ads} + H^+ + e^- \underset{k_{-2}}{\overset{k_2}{\rightleftarrows}} M + H_2 \quad (2)$$

(ii) chemical recombination (Tafel reaction), with rate v_3:

$$2MH_{ads} \underset{k_{-3}}{\overset{k_3}{\rightleftarrows}} 2M + H_2 \quad (3)$$

The adsorption reaction is followed by hydrogen absorption into a subsurface layer, with rate v_4:

$$MH_{ads} + M_{subsurface} \underset{k_{-4}}{\overset{k_4}{\rightleftarrows}} M_{surface} + MH_{abs}(subsurface) \quad (4)$$

and further diffusion into the bulk of metal:

$$MH_{abs}(subsurface) \overset{diffusion}{\longrightarrow} MH_{abs}(bulk) \quad (5)$$

as H_{abs} diffuses from one site M_1 to another M_2.

The model proposed in this paper contains two additional assumptions are considered:

- A direct absorption mechanism (7)–(9) [15] where the absorbed hydrogen in a subsurface layer is directly exchanged with protons in the solution bulk, with rate v_5:

$$H^+ + e \underset{k_{-5}}{\overset{k_5}{\rightleftarrows}} H^*_{abs} \quad (6)$$

- A possible exchange between the two types of absorbed hydrogen coming from the direct and indirect absorption:

$$H_{abs} \underset{k_r}{\overset{k_t}{\rightleftarrows}} H^*_{abs} \quad (7)$$

Then, this subsurface layer is richer in hydrogen, H_{abs} and H^*_{abs}, than the bulk phase where only H_{abs} is present.

2.2. Mathematical description of the model

The rates (mol cm^{-2} s^{-1}) of the above reactions can be written as

$$v_1 = k_1(1-\theta) - k_{-1}\theta \quad (8)$$

where θ is the surface coverage of the electrode surface by H_{ads}:

$$v_2 = k_2\theta - k_{-2}(1-\theta) \quad (9)$$

$$\nu_3 = k_3\theta^2 - 2k_{-3}(1-\theta) \tag{10}$$

$$\nu_4 = k_4\theta[1 - X(0)] - k_{-4}(1-\theta)X(0) \tag{11}$$

where $X(x) = c(x)/c_{max}$ is the dimensionless concentration of free H_{abs} in the metal with respect to the distance x to the electrode surface, and c_{max} is the maximum hydrogen concentration in the bulk of the metal. The concentrations of hydrogen ions and molecular hydrogen are included in the rate constants k_1 and k_{-3}, respectively.

The rate ν_5 is obtained from the flux, $J_t(x)$, of the "trapped" hydrogen atoms, H^*_{abs}, which cross the electrode surface:

$$\nu_5 = -J_t(0) \tag{12}$$

Then, if the various quantities are supposed to be only x-dependent:

$$\nu_5 = -\int_0^d \frac{\partial J_t(x)}{\partial x}\mathrm{d}x \tag{13}$$

However, as

$$c_{max}\frac{\partial X_t(x)}{\partial t} = -\frac{\partial J_t(x)}{\partial x} \tag{14}$$

where $X_t(x) = c_t(x)/c_{max}$ is the dimensionless concentration of H^*_{abs} "trapped" in the volume, V, of the metal film. $X_t(x)$ is supposed to depend on x only, hence:

$$\nu_5 = c_{max}\int_0^d \frac{\mathrm{d}X_t(x)}{\mathrm{d}t}\mathrm{d}x \tag{15}$$

The diffusion process in the iron film is supposed to be very fast compared to the rates of the surface and subsurface processes [16]. In the subsurface layer, a trapping/releasing process is supposed to occur such as

$$H_{abs} + \langle\,\rangle \underset{k_r}{\overset{k_t}{\rightleftarrows}} \langle H^*_{abs}\rangle \tag{16}$$

where $\langle\,\rangle$ represents an empty site and $\langle H^*_{abs}\rangle$ an occupied site by H^*_{abs} [17]; therefore, the kinetic equation which gives the change of the concentration of the H^*_{abs} is similar to the McKabb and Foster model [2]:

$$\frac{\partial X_t(x)}{\partial t} = \nu_t(x) + \nu_e(x) \tag{17}$$

where

$$\nu_t(x) = k_t X(x)[N(x) - X_t(x)] - k_r X_t(x) \tag{18}$$

is the rate of hydrogen trapping and $N(x)$ is the relative density of sites in the metal (i.e. the number per unit volume divided by c_{max}). And

$$\nu_e(x) = k_5[N(x) - X_t(x)] - k_{-5}X_t(x) \tag{19}$$

is the rate of exchange with the solution, whereas

$$\nu_5 = c_{max}\int_0^d \nu_e(x)\mathrm{d}x \tag{20}$$

is the exchange rate of the trapped hydrogen with the solution. Hence:

$$\nu_5 = c_{max}\int_0^d \{k_5[N(x) - X_t(x)] - k_{-5}X_t(x)\}\mathrm{d}x \tag{21}$$

In the previous equations, $k_i = k_i^0 \exp(b_i E)$ are in mol cm^{-2} s^{-1}, for $i = 1, -1, 2, -2$, and k_5, k_{-5}, k_t and k_r are in s^{-1}, $b_i = \pm\beta_i F/RT$, β_i is the symmetry coefficient of the reaction i, sign '$\pm$' is opposite sign of i, $X(0)$ is the hydrogen concentration just under the surface, $1 - X(0)$ is the dimensionless subsurface concentration of the free sites in the subsurface layer [18,19].

The faradaic cathodic current density is then equal to

$$j_F = -F(\nu_1 + \nu_2 + \nu_5) \tag{22}$$

In the same way the coverage changes of H_{ads} are described by

$$\Gamma_{max}\frac{\mathrm{d}\theta}{\mathrm{d}t} = \nu_1 - \nu_2 - 2\nu_3 - \nu_4 \tag{23}$$

where Γ_{max} is the density of adsorption sites on the metal surface (mol cm^{-2}).

The boundary conditions imposed to the metal film are the following:

- $x = 0$, the flux of the entering hydrogen in the film is equal to

$$J(0) = \nu_4 + \nu_5 \tag{24}$$

- $x = d$, the absorbed hydrogen atoms cannot cross the metal/gold interface, therefore:

$$J(d) = 0 \tag{25}$$

In the following, it is assumed that the sites are localized in the subsurface layer and have the relative density $N(x)$ which decreases exponentially with the distance from the electrode surface

$$N(x) = N_0 \exp\left(-\frac{x}{x_0}\right) \tag{26}$$

where $N_0 = c_{t,max}/c_{max}$ is the dimensionless subsurface concentration of the sites, relative to c_{max}, $c_{t,max}$ is the concentration of the occupied sites, and x_0 represents a characteristic distance of the sites, i.e. a distance where $N(x_0) = N_0/e$. This model is analyzed below, first in a steady state and later for impedance of an ion-blocking electrode constituted of an iron film of thickness d deposited on a gold substrate.

2.3. Steady state

The steady-state values of the surface coverage, θ, by adsorbed hydrogen, H_{ads}, and the dimensionless concentration of H species under the electrode surface, $X(0)$, are calculated following the simplifying assumption, that the Tafel desorption reaction is negligible ($k_3(E) = k_{-3}(E) = 0$) [2]:

At steady state, $\mathrm{d}/\mathrm{d}t \equiv 0$, then the hydrogen, H_{abs}, concentration is constant throughout the metal film as diffusion is supposed to be fast

From $v_1 - v_2 = v_4$:

$$\theta = \frac{k_1 + k_{-2} + k_{-4}X(0)}{k_1 + k_{-1} + k_2 + k_{-2} + k_4(1 - X(0)) + k_{-4}X(0)} \quad (27)$$

and from $v_1 - v_2 = -v_5$:

$$\theta = \frac{k_{-4}X(0) - v_5}{k_4(1 - X(0)) + k_{-4}X(0)} \quad (28)$$

where from Eq. (21):

$$v_5 = c_{\max} d\{k_5(1 - n) - k_{-5}n\}N^* \quad (29)$$

where

$$N^* = \frac{1}{d}\int_0^d N(x)\mathrm{d}x = N_0\frac{x_0}{d}\left[1 - \exp\left(-\frac{d}{x_0}\right)\right] \quad (30)$$

is the dimensionless total number of traps in the metal per volume unit (cm^{-3}) and $n = X_t(x)/N(x)$ is the fraction of occupied sites by hydrogen equal to

$$n = \frac{k_t X(0) + k_5}{k_r + k_t X(0) + k_5 + k_{-5}} \quad (31)$$

as from Eq. (17), $v_t + v_e = 0$ at steady state.

In the case considered here, where the density of sites decreases with depth, the "trapped" hydrogen atoms in these sites are located in a "subsurface layer" whose thickness can be considered as equal to two or three times x_0, and their total quantity in the electrode per volume unit is equal to

$$X^* = nN^* \quad (32)$$

By equating Eqs. (27) and (28), $X(0)$ is the solution of a quadratic equation such as

$$aX(0)^2 + bX(0) + c = 0$$

where

$$a = \gamma k_4(k_1 + k_{-2}) + \gamma k_{-4}(k_{-1} + k_2) - \alpha(k_{-4} - k_4),$$

$$b = \delta k_4(k_1 + k_{-2}) + \delta k_{-4}(k_{-1} + k_2) - \beta(k_{-4} - k_4) - \alpha(k_1 + k_{-1} + k_2 + k_{-2} + k_4) - \gamma k_4(k_1 + k_{-2}),$$

$$c = -\beta(k_1 + k_{-1}k_2 + k_{-2} + k_4) - \delta k_4(k_1 + k_{-2})$$

and

$$v_5 = \frac{\alpha X(0) + \beta}{\gamma X(0) + \delta} = c_{\max}N^*\frac{-k_t k_{-5}X(0) + k_r k_5}{k_t X(0) + k_r + k_5 + k_{-5}}$$

therefore

$$X(0) = -\frac{b \pm \sqrt{b^2 - 4ac}}{2a}$$

2.4. Small signal analysis

From Eqs. (22)–(24), the responses $\Delta\theta$, ΔI_F, $\Delta J(0)$, and $\Delta X(0)$ to a small amplitude sinusoidal potential perturbation ΔE are equal, in the frequency domain, to

$$\Delta j_F = -F(\Delta v_1 + \Delta v_2 + \Delta v_5) \quad (33)$$

where from Eqs. (21) and (29):

$$\Delta v_5 = c_{\max} d\{[b_5k_5(1 - n) - b_{-5}k_{-5}n]N^*\Delta E - (k_5 + k_{-5})\Delta X^*\} \quad (34)$$

where

$$\Delta X^* = \frac{1}{d}\int_0^d \Delta X_t(x)\mathrm{d}x \quad (35)$$

Hence

$$\Delta j_F = R_t^{-1}\Delta E + FK_I\Delta\theta + FK_5\Delta X^* \quad (36)$$

where

$$R_t^{-1} = -F[b_1k_1(1 - \theta) - b_{-1}k_{-1}\theta + b_2k_2\theta - b_{-2}k_{-2}(1 - \theta) + c_{\max}N^*(b_5k_5(1 - n) - k_{-5}b_{-5}n)] \quad (37)$$

and

$$K_I = k_1 + k_{-1} - k_2 - k_{-2} \quad (38)$$

$$K_5 = c_{\max}d(k_5 + k_{-5}) \quad (39)$$

and a small amplitude perturbation of the quantity X, is such as $\Delta X(t) = X(t) - X(\text{steady state})$. Therefore, the charge transfer resistance, R_t depends on the thickness of the metal film through $N^*(d)$ and θ (Eqs. (30) and (37)).

Similarly, from Eq. (23) it is possible to obtain

$$j\omega\Gamma_{\max}\Delta\theta = K\Delta E - K_0\Delta\theta + K_4\Delta X(0) \quad (40)$$

where

$$K = b_1k_1(1 - \theta) - b_{-1}k_{-1}\theta - b_2k_2\theta + b_{-2}k_{-2}(1 - \theta) \quad (41)$$

$$K_0 = k_1 + k_{-1} + k_2 + k_{-2} + k_4[1 - X(0)] + k_{-4}X(0) \quad (42)$$

$$K_4 = k_4\theta + k_{-4}(1 - \theta) \quad (43)$$

therefore

$$\Delta\theta = \frac{K\Delta E + K_4\Delta X(0)}{j\omega\Gamma_{\max} + K_0} \quad (44)$$

Finally, from Eq. (24):

$$\Delta J(0) = \Delta v_4 + \Delta v_5 \quad (45)$$

Hence

$$\Delta J(0) = K_1\Delta E + K_2\Delta\theta + K_3\Delta X(0) + K_5\Delta X^* \quad (46)$$

where

$$K_1 = c_{\max}dN^*(b_5k_5(1 - n) - b_{-5}k_{-5}n) \quad (47)$$

$$K_2 = k_4[1 - X(0)] + k_{-4}X(0) \quad (48)$$

$$K_3 = -K_4 \quad (49)$$

From Eq. (18), the response of the dimensionless "trapped" hydrogen concentration, ΔX_t, at a distance x from the electrode, is governed by

$$\frac{\mathrm{d}\Delta X_t}{\mathrm{d}t} = -(k_r + k_t X + k_5 + k_{-5})\Delta X_t + k_t[N(x) - X_t(x)]\Delta X \quad (50)$$

where X_t, ΔX_t, and ΔX are x-dependant, whereas $X = X(0)$, i.e. from Eq. (50):

$$j\omega\Delta X_t = -(k_r + k_t X(0) + k_5 + k_{-5})\Delta X_t + k_t \frac{k_r + k_{-5}}{k_t X(0) + k_5} X_t(x)\Delta X \quad (51)$$

therefore

$$\Delta X_t = \frac{k_t((k_r + k_{-5})/(k_t X(0) + k_5))X_t(x)\Delta X}{j\omega + k_r + k_t X(0) + k_5 + k_{-5}} \quad (52)$$

However from Eq. (35) and using Eq. (52):

$$\Delta X^* = \frac{1}{d}\int_0^d \frac{k_t(k_r + k_{-5})nN(x)\Delta X(x)}{(j\omega + k_r + k_t X(0) + k_5 + k_{-5})(k_t X(0) + k_r)}\mathrm{d}x \quad (53)$$

Therefore,

$$\Delta X^* = A\Delta X(0) \quad (54)$$

where

$$A = \frac{k_t(k_r + k_{-5})N_0 x_0(1 - \exp(-d/x_0))}{(j\omega + k_r + k_t X(0) + k_5 + k_{-5})(k_r + k_t X(0) + k_5 + k_{-5})} \quad (55)$$

However, as $\int_0^d (\partial\Delta J/\partial x)\,\mathrm{d}x = -c_{max}\int_0^d (\partial\Delta X/\partial t)\,\mathrm{d}x$, one has $\Delta J(0) = -j\omega d c_{max}\Delta X(0)$ and therefore

$$\Delta X(0) = -\frac{K_1\Delta E + K_2\Delta\theta}{j\omega d c_{max} + K_3 + AK_5} \quad (56)$$

From Eq. (44)

$$\Delta\theta = \frac{1/(j\omega\Gamma_{max} + K_0)(K - K_1K_4/(j\omega d c_{max} + K_3 + AK_5))}{1 + K_2K_4/(j\omega\Gamma_{max} + K_0)(j\omega d c_{max} + K_3 + AK_5))} \times \Delta E \quad (57)$$

On the other hand, using Eq. (54), and substitution of $\Delta X(0)$ by its value (Eq. (56)) into Eq. (36) the final form for ac current is obtained

$$\Delta j_F = \left(R_t^{-1} - \frac{FAK_5K_1}{j\omega d c_{max} + K_3 + AK_5}\right)\Delta E + F\left(K_I - \frac{FAK_5K_2}{j\omega d c_{max} + K_3 + AK_5}\right)\Delta\theta \quad (58)$$

Then the electrochemical admittance $Y_F = \Delta j_F/\Delta E$ of the hydrogen/electrode interface can be obtained by means of Eq. (57):

$$Y_F = R_t^{-1} - \frac{FAK_5K_1}{j\omega d c_{max} + K_3 + AK_5} + F\left(\frac{K_I - FAK_5K_2}{j\omega d c_{max} + K_3 + AK_5}\right) \times \frac{K - (K_1K_4)/(j\omega d c_{max} + K_3 + AK_5)}{j\omega\Gamma_{max} + K_0 + (K_2K_4)/(j\omega d c_{max} + K_3 + AK_5)} \quad (59)$$

This quantity can be obtained also by considering the value of the admittance calculated in Ref. [2] where diffusion has been supposed to be a rate limiting step and by assuming that the diffusion coefficient of hydrogen tends towards infinity. Then, in this limiting situation, the quantities $1/Q$ and W/Q involved in the calculated admittance [2], tend towards $-(j\omega d c_{max} + AK_5)$ and A, respectively, which lead to the same value as Eq. (59).

2.5. Predictions of the model

The impedance, $Z(\omega)$, and the change of the charge transfer resistance with respect to the thickness of the iron layer, d, was calculated from Eqs. (59) and (37), respectively (Fig. 2),

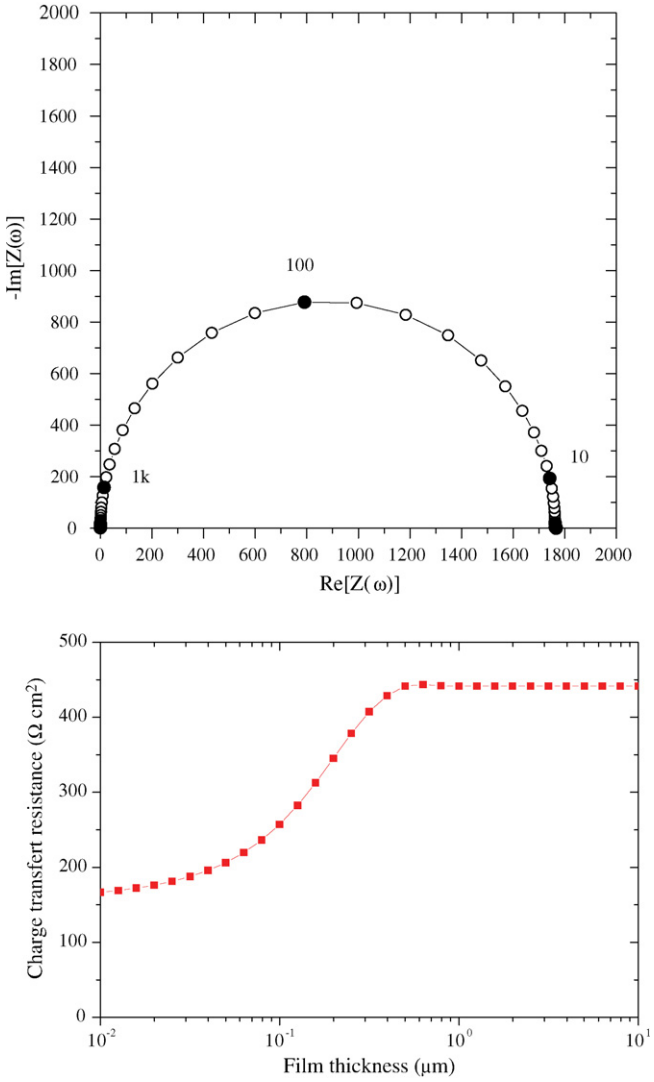

Fig. 2. Calculated (a) impedance (frequencies in Hz) and (b) charge transfer resistance change with respect to the thickness of the iron layer with the following parameters: $k_1(E) = 10^{-10}\exp(-20E)$ mol cm^{-2} s^{-1}, $k_{-1}(E) = 10^{-7}\exp(50E)$ mol cm^{-2} s^{-1}, $k_2(E) = 10^{-9}\exp(-10E)$ mol cm^{-2} s^{-1}, $k_{-2}(E) = 10^{-9}\exp(10E)$ mol cm^{-2} s^{-1}, $k_3 = 10^{-3}\exp(-20E)$ mol cm^{-2} s^{-1}, $k_{-3}(E) = 0$, $k_4(E) = 2\times10^{-5}$ mol cm^{-2} s^{-1}, $k_{-4}(E) = 10^{-5}$ mol cm^{-2} s^{-1}, $k_5(E) = 10^{-3}\exp(-25E)$ mol cm^{-2} s^{-1}, $k_{-5}(E) = 2\times10^{-8}\exp(10E)$ mol cm^{-2} s^{-1}, $k_t(E) = 10^3$ mol cm^{-3} s^{-1}, $k_d(E) = 0$, $N_0 = 5\times10^5$ mol cm^{-3}, $x_0 = 0.1$ μm, $c_{max} = 0.116$ mol cm^{-3}, $\Gamma_{max} = 7\times10^{-9}$ mol cm^{-2}, $C_d = 1$ μF.

for the values of the parameters given in the caption, in particular the ratio $k_5^0/k_{-5}^0 = 5 \times 10^{-4}$ was tested. The impedance, $Z(\omega)$, has the shape of a semi-circle when a double layer capacity is taken into account in parallel on the faradaic impedance, $Z_F(\omega)$ (Fig. 2a). The charge transfer resistance increases when the thickness of the iron film increases (Fig. 2b). This surprising behaviour is related to the dependence of R_t on the thickness of the iron film through N^* and n.

3. Experimental

In this experiment, the working electrode was made of a thin iron film, whose thickness changed from a few hundreds of nanometers to several micrometers, deposited on a gold electrode, 5 mm in diameter.

3.1. Electrodeposition of iron on a gold substrate

The main difficulty of this part of the work was to make iron deposits, which did not contain hydrogen and sufficiently adherent to allow impedance measurements to be performed. Hence, the gold disc electrode was very slightly rotated during electrodeposition not to facilitate the insertion of hydrogen in the deposit, which could be detrimental to the conclusions.

The electrodeposition solution was $FeSO_4{\cdot}7H_2O$ ($240\,g\,L^{-1}$), $FeCl_2{\cdot}4H_2O$ ($30\,g\,L^{-1}$) and NH_4Cl ($22.5\,g\,L^{-1}$). 0.1 M NaOH was added until the yellow colour turned to green blue, which corresponds to a solution pH between 4.5 and 6. The solution was maintained at 38 °C during electrodeposition. The counter electrode was a mild steel foil and the reference electrode was a mercurous/mercurous sulfate ($Hg/Hg_2SO_4/K_2SO_4$ saturated). The applied current density was between 50 and 100 mA cm^{-2}.

Before iron electrodeposition, the gold electrode was mechanically polished (600 and then 1200 emery paper grade), and then rinsed in deionized water and cleaned with ultrasounds in acetone. After electrodeposition, the composite electrode was rinsed in deionized water.

Gold was chosen as a substrate because it does not absorb hydrogen, then hydrogen entered and crossed the iron film and then was stopped by the gold substrate.

Fig. 3a and b shows the surface of the iron deposit observed by a scanning electron microscope. It demonstrates that gold is uniformly coated by the iron deposit both for a thin (0.44 μm) or a thicker (4.4 μm) film deposited on the gold surface.

3.2. Electrochemical cell

The experiments of hydrogen insertion on deposited iron on gold were carried out in 0.1 M H_2SO_4. A 5 mm diameter solid iron rotating disc electrode (Goodfellow) was also used to compare its characteristic to the iron film behaviour.

Electrochemical impedance measurements were carried out by using a frequency response analyzer (FRA: Solartron 1250) connected with a potentiostat (Solartron 1286). The amplitude of the perturbating sinusoidal signal was equal to 15 mV peak to peak in a 10 kHz to 100 mHz frequency range using 10 measurement points per decade.

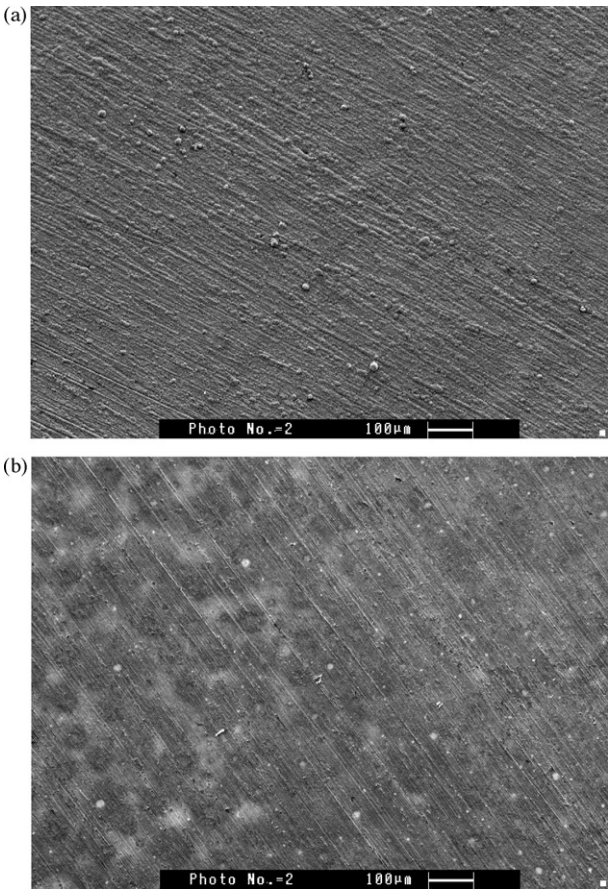

Fig. 3. Scanning electron microscopic observations of the surface of the iron films deposited on the gold electrode for thicknesses (a) 4.4 μm and (b) 0.44 μm.

Obtaining a steady state was particularly important to reach relevant quantities for impedance measurements. Then, it was necessary to wait a sufficient long time to reach a complete charging of hydrogen of the sample characterized by a steady-state current. In addition, it was necessary to impose an adequate hydrodynamic regime to eliminate the hydrogen bubbles generated at the interface.

Hydrogen bubble evolution perturbs the electrochemical measurements. When a rotating disc electrode is used, bubbles are blocked at the centre of the disc electrode as the active surface is oriented towards the bottom of the cell, the rotation axis being vertical. Therefore, the current and impedance measurements are difficult to achieve. To eliminate as quickly as possible the hydrogen bubbles, an impinging jet cell was used to decrease their influence on the experimental data. A fixed disc electrode at the bottom of the cell, vertically set to easily free the bubbles, was positioned under the electrolyte jet, which was horizontal. This type of cell ensures an uniform accessibility of the active species to the electrode surface. The volume of the electrolyte was about 1500 ml and the temperature of the solution was maintained at 25 °C. The counter electrode was a large area platinum grid and the reference electrode was a mercurous/mercurous sulphate electrode. The potential of the

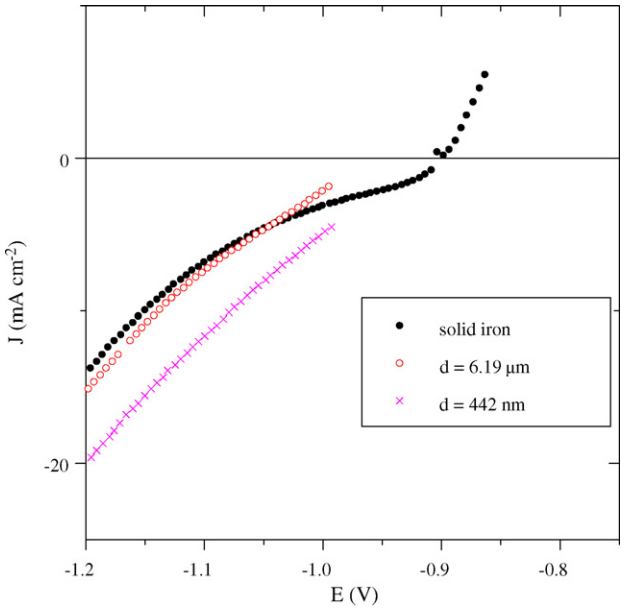

Fig. 4. Comparison of current–voltage curves obtained on solid iron electrode and deposited iron electrodes of various thicknesses in an impinging jet cell in 0.1 M H_2SO_4.

working electrode will be given, in the following, versus this reference electrode (SSE is +0.650 V with respect to the normal hydrogen electrode—NHE).

4. Results

The reactivity of the iron electrode and of the iron deposits on gold electrodes towards hydrogen was evaluated by using current–voltage curves in the cathodic domain in a first step and then their characterization was carried out by impedance measurements. The results were compared with the current–voltage curves and impedances obtained on a rotating iron disc electrode at a 2000 rpm rate.

4.1. Current–voltage curves

Current–voltage curves $I(E)$ were obtained by using a low potential sweep rate. Fig. 4 shows the comparison of the current–voltage curve of both the solid iron electrode and the deposited iron electrodes of various thicknesses in aerated 0.1 M H_2SO_4 (Fig. 4) medium. The curves are relatively close but the current was higher when the thickness of the iron deposit was lower. Measurements were also carried out in deaerated medium obtained by nitrogen bubbling but the difference due to oxygen reduction was small, then in the following the iron electrodepositions and their characterization were carried out in aerated media.

4.2. Electrochemical impedances

Before any impedance measurement, some time was necessary to reach a steady-state regime. This time corresponded to a complete charging of hydrogen in the iron film and depended on the imposed potential and the studied iron thickness. From the observed current transients, a 20 min delay was necessary for the solid iron electrode to reach a stable current before to carry out impedance measurements whereas a 60 min delay was necessary for iron deposited on gold.

Fig. 5 shows the impedance diagrams, measured at −1.1 V/SSE, for various thicknesses of the iron layer after stabilisation in a 0.1 M H_2SO_4 aqueous solution. Whatever the thickness of the iron layer deposited on the gold electrode or for a solid iron electrode the impedance diagrams were formed by an unique capacitive loop, which should represent the charge transfer resistance, R_t, in parallel on the double layer capacity, C_d. The main conclusion is that the charge transfer resistance changed with the thickness of the electrodeposited film. This demonstrated a surprising behaviour as, in principle, the charge transfer resistance characterizes solely surface phenomena and should not vary with the thickness of the tested sample.

Fig. 6 shows the change of R_t with respect to the thickness of the deposited iron film on a gold substrate at various potentials in a 0.1 M H_2SO_4 aqueous solution. After to be rather constant up to 1 μm, R_t increased with the thickness of the sample and asymptotically tended towards the value found for the charge transfer resistance of the solid iron electrode. For very thin films (smaller than 1 μm), R_t is constant, in agreement with the model prediction, as the surface charge transfer becomes preponderant and then independent of the thickness. For larger thicknesses (greater than 1 μm) an important increase of the R_t value was observed when the charge transfer in volume increases. For thicker iron films (greater than a few μm), R_t increased only a little bit as the charge transfer in volume is limited to a thin layer and finally tended towards an asymptotic line whose value was equal to the value obtained for a solid iron electrode.

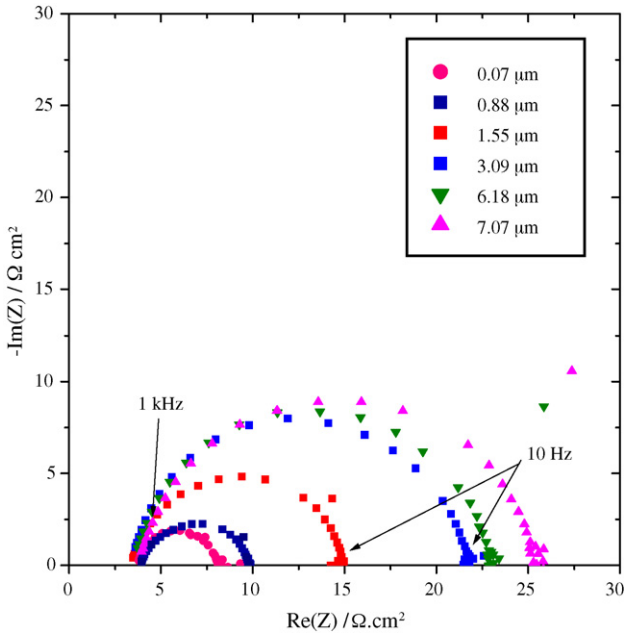

Fig. 5. Impedance diagrams measured on electrodeposited iron electrodes on a gold substrate in 0.1 M H_2SO_4 obtained in a impinging jet cell for various thicknesses in at −1.1 V/SSE (frequencies in Hz).

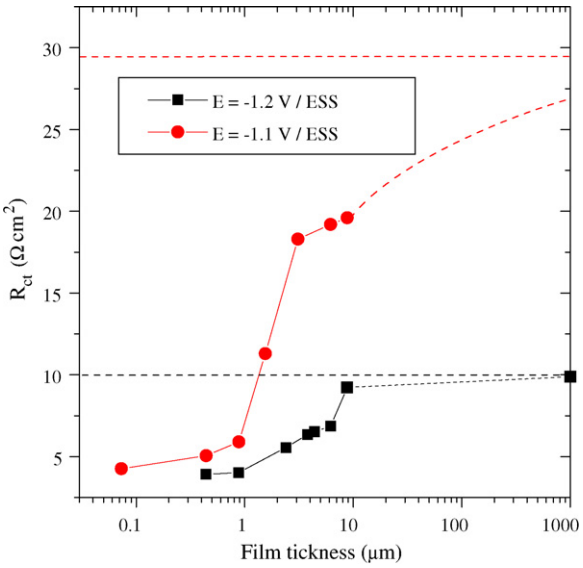

Fig. 6. Change of the charge transfer resistance with respect to the thickness of the iron deposited films on the gold electrode at −1.1 and −1.2 V/SSE and the limiting values (—) measured on a solid iron disc electrode of the electrodeposited iron at various potentials in 0.1 M H_2SO_4.

The change of R_t with respect to the potential is given in Fig. 7 for various thicknesses of the electrodeposited iron and for the solid iron electrode. For the latter, a large increase was observed for potential values lower than $E = -1.1$ V/SSE, whereas for the electrodeposited iron electrodes the charge transfer resistance increased between $E = -1.2$ and -1.1 V/SSE and then slightly decreased probably due to the growing influence of the anodic process. This increase was as much important as the deposit was thicker. For more cathodic potentials, the value of the charge transfer resistance decreases proportionally to the inverse of the cathodic current.

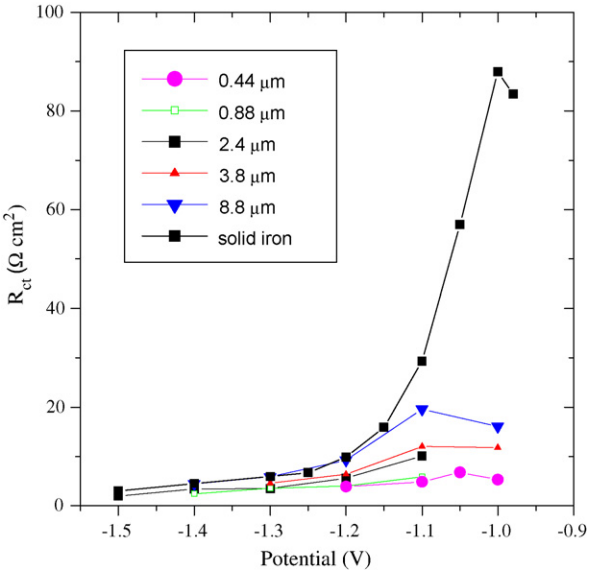

Fig. 7. Change of the charge transfer resistance with respect to the potential for various thicknesses of the electrodeposited iron in 0.1 M H_2SO_4.

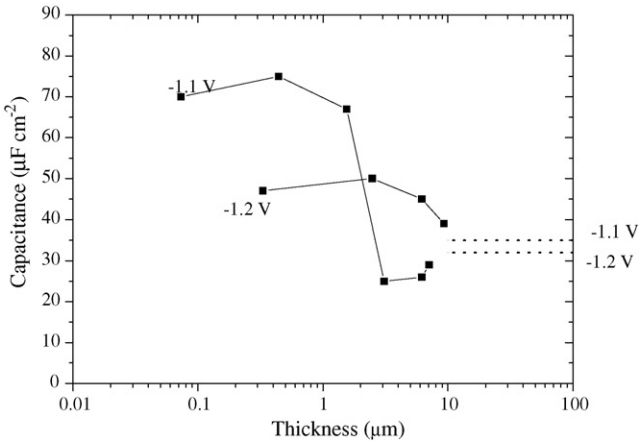

Fig. 8. Change of the double layer capacitance with respect to the thickness of the iron deposited film on the gold electrode.

5. Discussion

The main experimental result of this study is the thickness dependence of the charge transfer resistance of the impedance of the iron film electrode. As, usually, this resistance is independent of the substrate volume as it is a surface dependent quantity, it is necessary to check that this surprising increase of the charge transfer resistance was not due to the decrease of the roughness of the iron film surface. Fig. 8 shows the variation of the double layer capacitance with respect to the thickness of the iron layer and the limiting value obtained for a solid iron electrode obtained from the impedance measurements. In fact, this capacitance decreases when the thickness of the film increases showing that the active surface is lower for thick films probably due to a rougher deposit for the thinner films. The active surface was about two times smaller for thick deposits than for thin deposits, which explains why the current is larger for thin deposits in Fig. 4. However, the increase of the charge transfer resistance is more than three times from thin to thick deposits, which demonstrates that the increase of this resistance is not due only to a change of active surface.

To interpret the R_t thickness dependence it is necessary to consider, in addition to a classical charge transfer at the electrode surface an extra charge transfer involving the bulk metal. Then, it is proposed here to consider the competition of two insertion processes of hydrogen in the iron film, which occur in parallel and schematized in Fig. 7. The first one is the classical two-step indirect absorption process, via the H_{ads} adsorbed intermediate, first proposed by Bockris et al. [20], whose rate constants are k_1, k_{-1}, k_4, k_{-4}. The second one can be seen as a generalization of the one-step Frumkin direct insertion process [21–23], which generates the H^*_{abs} in a thin sublayer, which was already proposed for the Pd/H system, and whose rate constants are k_5, k_{-5}. In the sublayer, the absorbed monoatomic hydrogen, H_{abs}, and the "trapped" hydrogen, H^*_{abs}, are supposed to interact through k_t, k_r. On these basis, the model proposed in the first part of this paper predicts that the charge transfer resistance is film thickness-dependent if either k_5 or k_{-5} is not

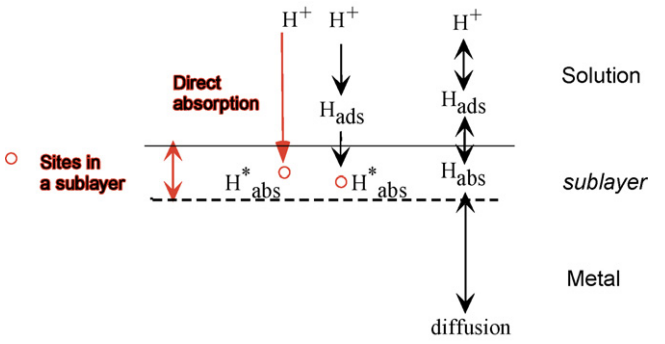

Fig. 9. Scheme of the reaction mechanism proposed for the interaction of hydrogen with iron.

zero. In addition, if $k_5 = 0$, then k_t, k_4, and k_5 have not to be equal to zero and if $k_{-5} = 0$, k_r and k_5 have not to be equal to zero.

Now, when $k_{-5} = 0$ the charge transfer resistance is always increasing with the iron film thickness whatever the values of the other rate constants. When $k_5 = 0$, the charge transfer resistance decreases when the film thickness increases. This means that for iron a direct absorption of hydrogen has to be considered to fit the experimental increase of R_{ct} when d increases (at least $k_5(E) \gg k_{-5}(E)$ is needed). As a comparison, for palladium this is $k_{-5}(E) \gg k_5(E)$ which is necessary, as the charge transfer resistance is decreasing when the palladium film thickness increases.

When $k_{-5} \neq 0$, the sense of variation of the charge transfer resistance with respect to the film thickness depends of the values of k_1 and k_{-1} whatever the value of k_5.

Finally, the reaction mechanism proposed in this paper to describe the interaction of hydrogen with iron is depicted in Fig. 9.

Usual kinetic models, where charge transfer is supposed to occur only on the electrode surface, lead to charge transfer resistances independent of the thickness of the specimen. In this paper, to account for the thickness dependence of the charge transfer resistance, it was supposed that charge transfer occurs in a sublayer inside the sample as well. It was assumed that hydrogen atoms were bonded on some sites with an exponential distribution from the electrode surface. These sites can be generated by the coexistence of hydrogen-rich zones in the sublayer and hydrogen-poor zones in the deep bulk of the film. They can be different from the commonly considered traps, which are generated by compressive stresses, grain boundaries or dislocations. Notice that the hypothesis of the existence of two types of hydrogen bonded to the metal lattice have been already considered in the literature (e.g. H and H* in [24,25]). However, a model taking into account only an heterogeneity of 2D adsorption sites will not be able to explain such a thickness-dependence of the charge transfer resistance.

Two other types of adsorbed hydrogen are also considered: H_{UPD} and H_{OPD} in [26,27], H_{UPD} being right on the metal surface and H_{OPD} adsorbed on the second layer. The second type is sometimes considered as due to the direct absorption as it "undergoes direct interfacial transfer to a subsurface site, followed by transfer to an interstice below the second surface monolayer becoming absorbed H" [28,29]. However, this view is only valid for monocrystals. In fact, even when the deposit is made on Au(1 1 1) like in Ref. [9], the first layers are not perfect, because there is not a layer-by-layer deposit at the beginning due to the misfit between the lattice of gold and palladium [30]. So, Lasia has noted that more than two monolayers are necessary to get normal absorption, i.e. H_{abs}. In the present experiment, where iron (and probably palladium in [31]) was electrochemically deposited on polycrystalline gold, numerous layers of the deposited metal were probably perturbed before to reach a more homogeneous structure. This could explain why the direct absorption mechanism is not limited to a depth equal to two monolayers as in perfect crystals, but can go much deeper in the bulk metal (here a few micrometers). This argument can be related to an hypothesis made by Bucur [32], on the possibility of two kinds of adsorption sites of hydrogen on palladium: a weak adsorption site on the crystallographic planes at the surface of palladium and strong adsorption sites on the surface imperfections, which can be distributed in the whole volume of the palladium. He has supported this assumption by the findings that on an ideal surface of a palladium monocrystal only the weak adsorbed species can be identified [33], while on black palladium a quite wide spectrum of strongly bonded forms can be found [34].

As the proposed model is not obviously unique, another possible model, which would have a similar behaviour, would be to consider a uniform "trap" density in the bulk metal and rate constants k_5 and k_{-5} which would decrease exponentially with the distance from the surface due to a gradient of physical properties of the metal. It would give very close predictions on R_t, as the mathematics are similar, because k_5, k_{-5} and N^* appear as products k_5N^* and $k_{-5}N^*$ in the expression of the charge transfer resistance (Eq. (37)).

6. Conclusion

The main result of this study, which characterizes the hydrogen interaction with iron, is that the charge transfer resistance increases with the film thickness on the opposite of the behaviour of the transfer resistance measured on palladium films [31]. A model taking into account the classical two-step indirect insertion of hydrogen into iron in competition with a direct entry of hydrogen in the iron electrode of absorbed monoatomic hydrogen in sites in a sublayer is proposed.

These experiments on the hydrogen/iron system allow the behaviour of iron to be compared, at least qualitatively, to the behaviour of palladium concerning its interaction with hydrogen when the metal is deposited in thin films on a gold substrate. However, it is necessary to keep in mind that for iron, hydrogen is evolving under bubble form in the whole cathodic range whereas there is solely absorption in the potential range of the α-phase for palladium. A variation of the charge transfer resistance with respect to the thickness of the film is observed for the two metals. This feature is highly surprising as the charge transfer resistance is generally related to surface phenomena and not to volume processes. This special behaviour has been explained by

a "trapping" of the absorbed hydrogen in a sublayer just below the surface of the electrode and, for palladium, a direct desorption of this "trapped" hydrogen in the solution [31]. However, for palladium, the charge transfer resistance decreases when the thickness of the film increases whereas for iron this resistance increases with the thickness of the film, which was explained by a direct absorption of hydrogen on the sites in the sublayer. Therefore, the involvement of a one-step Frumkin mechanism of direct hydrogen absorption is responsible for the observed interaction of hydrogen with palladium and iron. At the end, a possible explanation of such a deep penetration of the direct hydrogen absorption in the metal is proposed. It is based on the imperfections of the first layers of the deposited metals on polycrystalline gold.

Acknowledgments

The authors gratefully acknowledge the financial support of IFREMER. They thank Dr D. Festy for valuable discussions.

References

[1] S.I. Pyun, T.H. Yang, J. Electroanal. Chem. 441 (1998) 183.
[2] A. McNabb, P.K. Foster, Trans. Met. Soc. AIME 227 (1963) 618.
[3] T.H. Yang, S.I. Pyun, Electrochim. Acta 41 (1996) 843.
[4] C. Montella, J. Electranal. Chem. 497 (2001) 3.
[5] P.P. Grand, PhD Thesis, Université de Sherbrooke and Université de Pierre et Marie Curie, Paris, 2001.
[6] C. Gabrielli, P.P. Grand, A. Lasia, H. Perrot, J. Electrochem. Soc. 151 (2004) A1925.
[7] A. Lasia, J. Electroanal. Chem. 593 (2006) 159.
[8] L. Birry, A. Lasia, Electrochim. Acta 54 (2006) 3356.
[9] H. Duncan, A. Lasia, Electrochim. Acta 52 (2007) 6195.
[10] T. Zakroczymski, J. Flis, Electrochim. Acta 41 (1996) 1245.
[11] P. Bruzzoni, R.M. Carranza, J.R.C. Lacoste, Int. J. Hydrogen Energy 24 (1999) 1093.
[12] M.H. Abd Elhamid, B.G. Ateya, K.G. Weil, H.W. Pickering, J. Electrochem. Soc. 147 (2000) 2148.
[13] F.M. Al Faqeer, K.G. Weil, H.W. Pickering, Electrochim. Acta 48 (2003) 3565.
[14] Z. Wolarek, T. Zakroczymski, Acta Mater. 52 (2004) 2637.
[15] J.S. Chen, J.P. Diard, R. Durand, C. Montella, J. Electroanal. Chem. 406 (1996) 1.
[16] B.G. Pound, in: J. O'M Bockris (Ed.), Modern Aspects of Electrochemistry, vol. 25, Plenum Press, New York, 1993, p. 63.
[17] J.P. Diard, C. Montella, J. Electroanal. Chem. 557 (2003) 19.
[18] A. Lasia, D. Grégoire, J. Electrochem. Soc. 142 (1995) 3393.
[19] S.Y. Qian, B.E. Conway, G. Jerkiewicz, J. Chem. Soc., Faraday Trans. 94 (1998) 2945.
[20] J. O'M Bockris, J. McBreen, L. Nanis, J. Electrochem. Soc. 112 (1965) 1025.
[21] I.A. Bagotskaya, Zh. Fiz. Khim. 36 (1962) 2667.
[22] A.N. Frumkin, in: P. Delahay (Ed.), Advances in Electrochemistry and Electrochemical Engineering, vol. 3, Interscience Pub, New York, 1963, p. 287.
[23] G. Zheng, B.N. Popov, R.E. White, J. Electrochem. Soc. 142 (1995) 154.
[24] B. Béchet, I. Epelboin, M. Keddam, J. Electroanal. Chem. 76 (1977) 129.
[25] I. Epelboin, Ph. Morel, H. Takenouti, J. Electrochem. Soc. 118 (1971) 1282.
[26] B.E. Conway, G. Jerkiewicz, J. Electroanal. Chem. 357 (1993) 47.
[27] M.E. Martins, C.F. Zinola, G. Andreasen, R.C. Salvarezza, A.J. Arvia, J. Electroanal. Chem. 445 (1998) 135.
[28] G. Jerkiewicz, A. Zalfaghari, J. Electrochem. Soc. 143 (1996) 1240.
[29] M.V. Vigdorovich, V.I. Vigdorovich, L.E. Tsygankova, J. Electroanal. Chem. 596 (2006) 1.
[30] E. Budevski, G. Staikov, W. J. Lorenz, Electrochemical Phase Formation and Growth, VCH, Weinheim, p. 410.
[31] C. Gabrielli, P.P. Grand, A. Lasia, H. Perrot, J. Electrochem. Soc. 151 (2004), A1925, A1937, A1943.
[32] R.V. Bucur, Surf. Sci. 62 (1977) 519.
[33] H. Conrad, G. Ertl, E.E. Lutta, Surf. Sci. 41 (1974) 435.
[34] L.V. Babenkova, N.M. Popova, D.V. Sokoiskii, V.K. Solnyshkova, Dokl. Akad. Nauk. SSSR 210 (1973) 888.